

Experimental investigation of wind-induced internal pressures in nominally sealed building structures^{*}

Xian-feng YU¹, Jing-xuan GAO¹, Zhuang-ning XIE^{†‡1}, Xu WANG²

¹State Key Laboratory of Subtropical Building Science, South China University of Technology, Guangzhou 510640, China

²State Key Laboratory Breeding Base of Mountain Bridge and Tunnel Engineering, Chongqing Jiaotong University, Chongqing 400074, China

[†]E-mail: znxie@scut.edu.cn

Received Mar. 10, 2019; Revision accepted May 30, 2019; Crosschecked June 6, 2019

Abstract: The action of internal pressure cannot be neglected in wind-resistant design of large-span structures, high-rise buildings, and low-rise residential buildings. In this study, the internal pressure characteristics were first measured in still air in a completely closed building structure without any leakage. Then a series of wind tunnel tests were conducted to study the probability density distribution characteristics of the internal pressure responses in a nominally sealed building with background leakage. The mean and peak internal pressure responses associated with different background leakage distributions and wind directions were further investigated, and the experimental results were compared with those suggested by the Chinese wind load code GB50009-2012. The results indicated that the internal pressure in the completely closed building was non-stationary, and varied significantly when collected at different time points. Furthermore, a period of about 24 h was observed from the measured time history of internal pressure over 9 d. The internal pressure in a nominally sealed building structure nearly fitted a normal Gaussian distribution. When background leakage was uniformly arranged on the surface of the building, the mean internal pressure coefficient remained unchanged with increasing background leakage, varying within the range from -0.15 to -0.14 , indicating lower magnitudes than the value of -0.2 suggested by the Chinese wind load code. The minimum negative peak internal pressure coefficient was -0.255 when the peak factor was 3.5, indicating a lower magnitude than the value of -0.326 calculated in the Chinese wind load code.

Key words: Internal pressure; Wind tunnel experiment; Completely closed; Nominally sealed; Background leakage
<https://doi.org/10.1631/jzus.A1900091>

CLC number: TU312.1

1 Introduction


Internal pressure is an inevitable problem in wind-resistant design of large-span structures, high-rise buildings, and low-rise residential buildings. Wind engineering researchers have studied this area for many years, focusing mainly on theoretical re-

search (Holmes, 1979; Sharma and Richards, 1997; Yu et al., 2008; Guha et al., 2011) and wind tunnel experiment studies (Yu et al., 2006; Oh et al., 2007; Pan et al., 2013; Yu, 2016) of the steady-state internal pressure of rigid single-cell buildings with dominant openings. When background leakage and roof flexibility are considered, the internal pressure governing equation can be further developed. Its effectiveness and precision have been verified through wind tunnel tests.

In respect of a multi-room building with a windward dominant opening and a partition wall opening, Saathoff and Liu (1983) indicated that the governing equation of steady-state internal pressure could be established for each opening, so that the

[‡] Corresponding author

^{*} Project supported by the Fund of State Key Laboratory of Subtropical Building Science, South China University of Technology, China (No. 2019ZB28) and the Key Project of Foundation and Frontier Research of Chongqing, China (No. cstc2017jcyjAX0187)

 ORCID: Xian-feng YU, <https://orcid.org/0000-0002-3047-4886>

© Zhejiang University and Springer-Verlag GmbH Germany, part of Springer Nature 2019

time-varying internal pressure response for each room could be obtained. However, the governing equation they adopted still had some limitations. For a two-compartment building, a loss coefficient was introduced to describe the damping characteristics of an orifice, then more appropriate governing equations were developed (Guha et al., 2013a). After taking background leakage into account, the governing equations of internal pressure were further improved (Yu et al., 2012, 2019).

In respect of wind-induced internal pressure overshoot in a building with an opening, a specially designed polyethylene membrane was used by Stathopoulos and Luchian (1989) to simulate the sudden breakage of a window or door. Experimental results showed that the transient overshooting of internal pressure was not as high as the subsequent steady-state peak fluctuations. The same conclusion was reached by Tecle et al. (2013), who used a digital servo motor system to simulate the sudden failure of a door or window during wind tunnel tests. However, they indicated that the limited time response of the opening mechanism might be a reason why significant overshooting was neither expected nor observed. Later, Guha et al. (2013b) numerically investigated the transient response of internal pressure following the creation of a sudden opening. They showed that significant overshooting of internal pressure, higher than the subsequent steady-state resonant values, was possible when the opening was created almost instantaneously during the occurrence of high external pressure nearby.

Although wind engineering researchers have investigated steady-state and transient wind-induced internal pressure responses using wind tunnel experiments and numerical simulation, few studies have examined the internal pressure characteristic of a completely closed building structure. Neither have there been systematic investigations of the internal pressure response in a nominally sealed building with background leakage. Internal pressure in a nominally sealed building has been considered to some extent when studying the internal pressure of a building with a dominant opening. Ginger et al. (1997) conducted full-scale measurement of internal pressure for a typical nominally sealed low-rise building, and pointed out the mean internal pressure coefficient was

-0.14 and the internal pressure fluctuations were significantly lower than the external pressure fluctuations. Internal pressure fluctuation above the characteristic frequency was attenuated. Wind tunnel experiments were carried out by Oh et al. (2007) to investigate the internal pressure characteristics of a low-rise building with only leakages (nominally sealed building) or with a dominant opening. The maximum internal pressure coefficient was 0.1 in the nominally sealed case. Kopp et al. (2008) also indicated that the maximum internal pressure coefficient of a nominally sealed building would never be above 0.1.

The internal pressure characteristics of a completely closed building formed the basis of this study of the wind-induced internal pressure response of a nominally sealed building. If quantified leakage holes are arranged on the surface of a completely closed building, the leakage ratio can be exactly defined. Currently, studies of the mean and peak internal pressure responses in a nominally sealed building with an exact background leakage ratio are of great practical value to the wind-resistant design of both long-span structures and low-rise residential buildings. Generally, external pressure distributions are always obtained by wind tunnel experiments, while the internal pressure is determined according to wind load codes rather than wind tunnel tests. As for a nominally sealed building, the mean internal pressure coefficient is ± 0.2 , and the peak internal pressure coefficient is ± 0.326 at the reference height of 20 m in terrain category B, when the gust effect is considered, according to the Chinese load code GB50009-2012 (MOHURD, 2012) for the design of building structures. However, the rationality of the internal pressure value suggested by the load code is directly associated with the safety and economy of building structures.

In this study, the internal pressure characteristics of a completely closed building were first investigated. Then, the probability density distribution of the fluctuating internal pressure in a nominally sealed building was studied to determine a method for calculating the peak internal pressure. Finally, the mean and peak internal pressures were investigated in detail under different background leakage conditions, and a comparison of our results with the values suggested by wind load code is discussed.

2 Experimental setup

A 1:100 scale model of a typical large-span building (such as a single-story industrial building) was constructed with plexiglass plate of 5 mm thickness, and two lateral rib stiffeners were applied to ensure enough strength and stiffness. The dimensions of the prototype building were 80 m×40 m×20 m for length, width, and height, respectively. The maximum leakage area was determined according to the definition of the absolute background leakage ratio (ε) suggested by Ginger et al. (1997) as follows:

$$\varepsilon = \frac{\text{Effective leakage area}}{\text{Surface area of the building}} \in [10^{-4}, 10^{-3}]. \quad (1)$$

For this model with a total surface area of $8 \times 10^5 \text{ mm}^2$, the maximum leakage area was 800 mm^2 . Background leakage was simulated by 114 circular holes each with a diameter of 3 mm. All the circular holes were uniformly arranged on the four walls rather than the roof, considering rain-resistant design, so 39 holes were arranged on each front and back wall and 18 on each of the left and right walls. In addition, one internal tap was installed at the bottom of the model (Fig. 1).

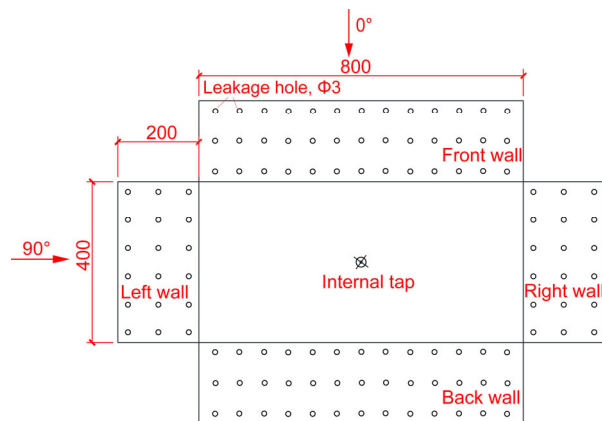


Fig. 1 Exploded view of the wind tunnel model sketch showing basic dimensions, locations of leakage holes and internal tap, and wind direction (unit: mm)

To systematically investigate the internal pressure responses in a nominally sealed building under different background leakages, 70 work cases were conducted (Table 1). In cases 1 to 8, the effects of different uniform leakage ratios on internal pressure

were studied. In cases 9 to 23, the effects of leeward wall leakage ratios on internal pressure were investigated when the leakage holes in the front wall were half opened uniformly. The effects of windward wall leakage ratios on internal pressure were studied in cases 24 to 38 when the leeward wall leakage holes were half opened. Cases from 39 to 53 were designed to obtain the unfavorable negative internal pressure. The variation of internal pressure with wind direction was investigated in cases 54–60 and 61–70 when the leakage holes in each wall were all opened and half opened, respectively.

Wind tunnel tests were performed in the boundary layer wind tunnel at the South China University of Technology, China. The test section is 5.4 m wide and 3 m high. Terrain category B with a power law exponent of 0.15, which stands for a suburban flat terrain, was simulated according to the Chinese load code (GB50009-2012) for the design of building structures. The simulated normalized velocity profile (V/V_H), turbulence intensity distribution (I_u), and power spectrum density (S_u) of approaching wind at roof height (H) are shown in Fig. 2, where V_H and σ_u are the mean value and standard deviation of the approaching wind velocities, respectively. L_u is the turbulence integral scale at roof height. V, f , and Z are the approaching wind velocity, frequency, and height, respectively. Fig. 3 presents an image of the wind tunnel and building model. To improve the experimental precision, the mean internal pressure and reference wind velocity were obtained using three pressure sensors (No. 9033) with calibration precision from the Pressure Systems Incorporation (PSI), USA. The sampling frequency was 10 Hz. Fluctuating internal pressure was obtained by pressure sensor “measurement” with a sampling frequency of 330 Hz. This sensor was also made by the PSI. The reference wind velocity at roof height was about 7.2 m/s. The test sampling time was 62.06 s, so amount of data of the internal pressure tap was up to 20480.

To conduct comparative analysis, another 1/200 scale model was constructed to simulate a super large-span building (such as exhibition center). The prototype building was 280 m×140 m in plan and 40 m in height. Background leakage holes were uniformly arranged on the surface of the model, and the maximum absolute leakage ratio ε was 10^{-3} . Then, wind tunnel tests were carried out according to some of the cases shown in Table 1. The simulated wind

Table 1 Experimental cases

Case	Leakage ratio, η (%)				Wind direction ($^\circ$)
	Front wall	Back wall	Left wall	Right wall	
1	12.5	12.5	12.5	12.5	0
2	25	25	25	25	0
3	37.5	37.5	37.5	37.5	0
4	50	50	50	50	0
5	62.5	62.5	62.5	62.5	0
6	75	75	75	75	0
7	87.5	87.5	87.5	87.5	0
8	100	100	100	100	0
9–23	50	0–100	0	0	0
24–38	0–100	50	0	0	0
39–53	0–100	100	100	100	0
54–60	100	100	100	100	0–90
61–70	50	50	50	50	0–90

Note: leakage ratio η indicates the number of opened holes in the wall/the total number of holes in the wall

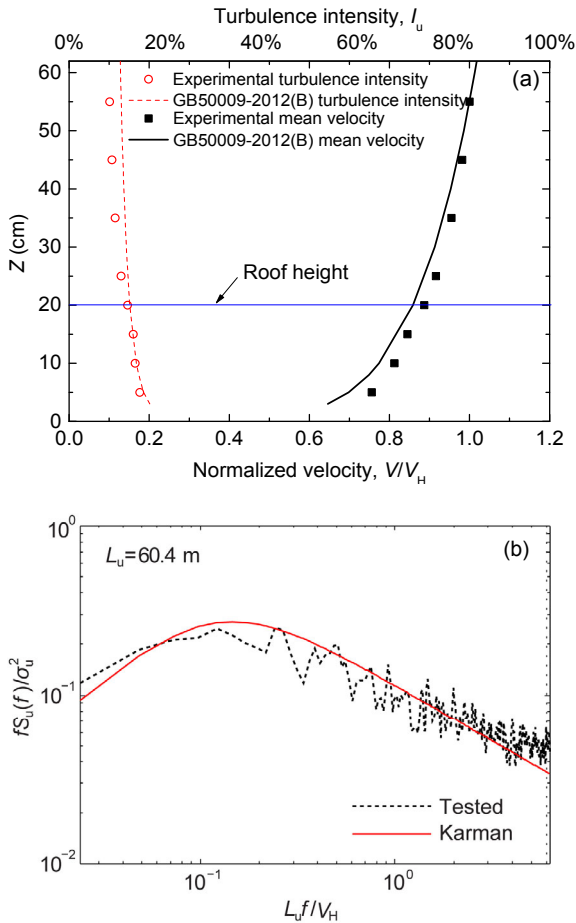


Fig. 2 Simulated wind parameters

(a) Mean velocity profile and turbulence intensity distribution; (b) Power spectrum density of approaching wind at roof height (scale 1/100)



Fig. 3 Image of the wind tunnel and building model (scale 1/100)

parameters are presented in Fig. 4, and an experimental model image is shown in Fig. 5.

Assuming that the time history of internal pressure at the internal tap is $P_i(t)$, the non-dimensional internal pressure coefficient $C_{pi}(t)$ can be expressed as

$$C_{pi}(t) = \frac{P_i(t) - P_\infty}{0.5 \rho_a V_H^2}, \quad (2)$$

where P_∞ is the static pressure, ρ_a is the air density, and V_H is the mean reference wind velocity at roof height. Then, the mean internal pressure coefficient \bar{C}_{pi} and

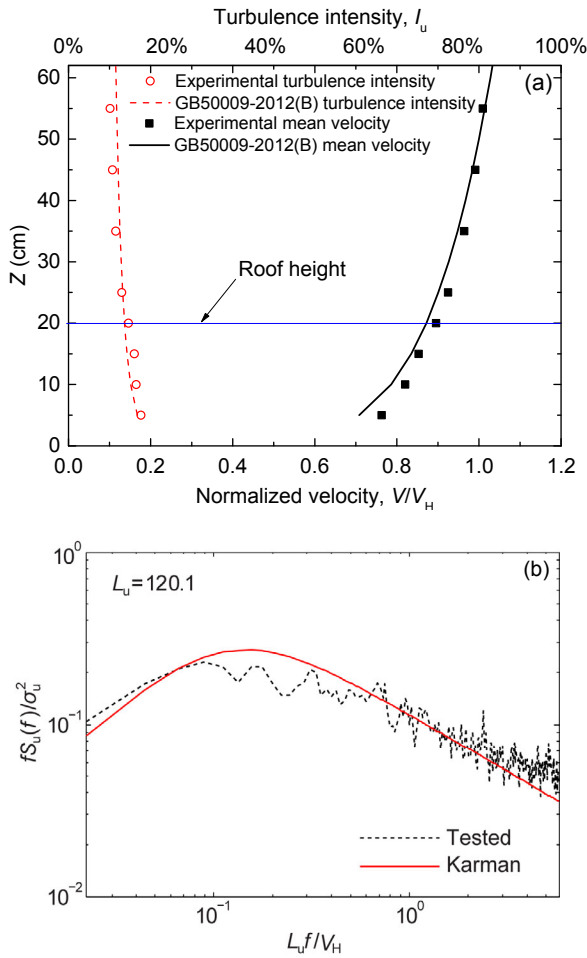


Fig. 4 Simulated wind parameters for large-span building model
 (a) Mean speed profile and turbulence intensity distribution;
 (b) Power spectrum density of approaching wind at roof height (scale 1/200)

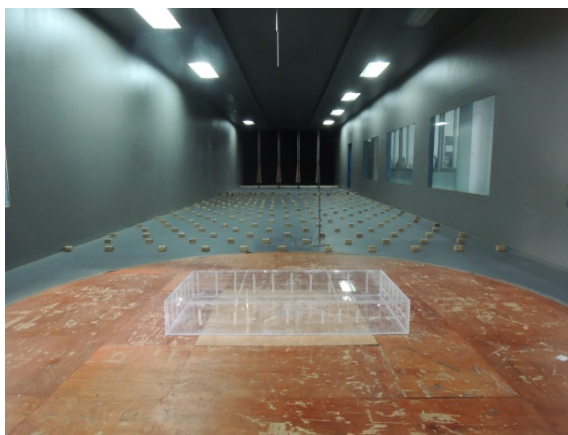


Fig. 5 Image of the wind tunnel and a large-span building model (scale 1/200)

the standard deviation of the internal pressure coefficient \tilde{C}_{pi} are as follows:

$$\bar{C}_{pi} = \frac{1}{N} \sum_{j=1}^N C_{pi,j}, \quad (3)$$

$$\tilde{C}_{pi} = \sqrt{\frac{1}{N-1} \sum_{j=1}^N (C_{pi,j} - \bar{C}_{pi})^2}, \quad (4)$$

where $C_{pi,j}$ is the j th value of the time history of internal pressure coefficient, and the amount of sampling data $N=20480$.

3 Results and discussion

A building in a nominally sealed condition is relative to the state of completely closed, so it is necessary first to investigate the internal pressure characteristics of a completely closed building. In this section, the internal pressure characteristics of a completely closed building are first discussed, then a quantitative analysis of the mean and peak values of the internal pressure response for buildings with background leakage (i.e. in a nominally sealed condition) is described.

3.1 Completely closed building

The measured time histories of internal pressure in the completely closed building model with dimensions $80 \text{ cm} \times 40 \text{ cm} \times 20 \text{ cm}$ are shown in Fig. 6. The results indicate that the internal pressure of a completely closed building is non-stationary. The internal pressures collected at different time points vary significantly, and the time histories of internal pressure are very similar to those when the internal tap is blocked. Therefore, once the observed time history of internal pressure is similar to that shown in Fig. 6 when the internal tap is unblocked, it can be concluded that the building model is completely closed without any background leakage.

The variation of internal pressure in a building model changing from a completely sealed state to a nominally sealed state is presented in Fig. 7. The internal pressure is non-stationary within the first 24 s, and then decreases to zero rapidly when a leakage hole occurs at 24 s. Fig. 8 illustrates a comparative analysis of the internal pressures in completely closed

and nominally sealed building models. The internal pressure in the nominally sealed building model fluctuates slightly around zero, while in the completely closed model it fluctuates significantly and shows an increasing trend over the whole 3-min timeframe.

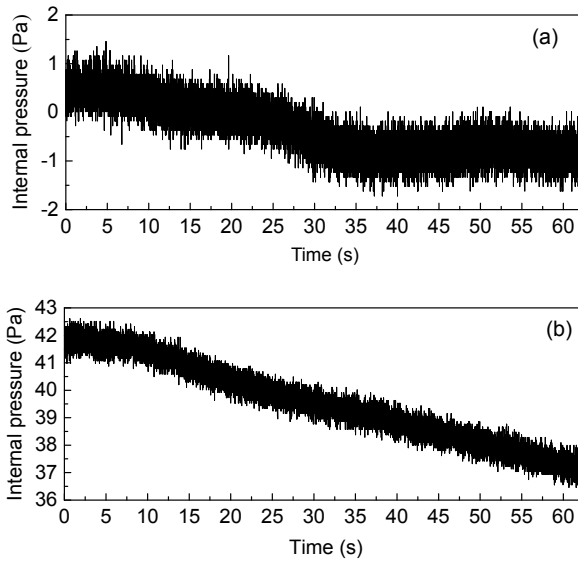


Fig. 6 Time history of internal pressure in a completely closed building model

(a) Collected the first time; (b) Collected the second time

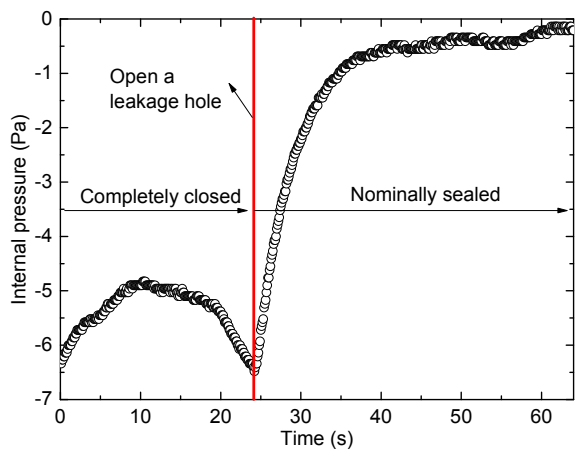


Fig. 7 Variation of internal pressure in a building model from a completely closed state to a nominally sealed state

To further explore the variation of internal pressure in a completely closed building over a relatively long time, internal pressure was sampled for up to 9 d in a silent environment in a completely closed

building model. The sampling frequency was set as 1 Hz. The measured time history of internal pressure plotted in Fig. 9 shows that: (1) The internal pressure shows an increasing trend on the whole, with a maximum internal pressure of 2.2 kPa and a minimum internal pressure of -0.25 kPa. (2) A period of about 24 h is observed from the internal pressure time history, which suggests that the internal pressure in a completely closed building might be related to the ambient temperature. (3) On the 9th day, the internal pressure rapidly decreased to zero when a leakage hole was opened and a very strong air jet could be heard.

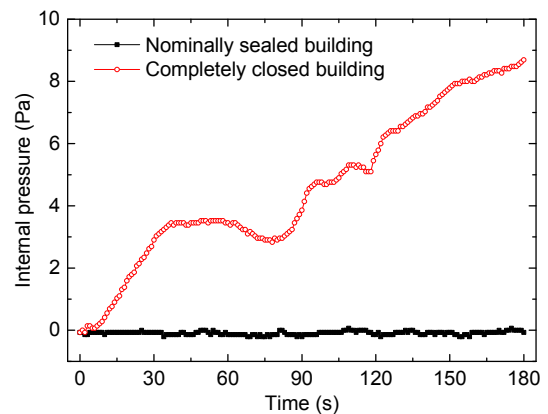


Fig. 8 Comparative analysis of the internal pressures in a completely closed building model and a nominally sealed building model

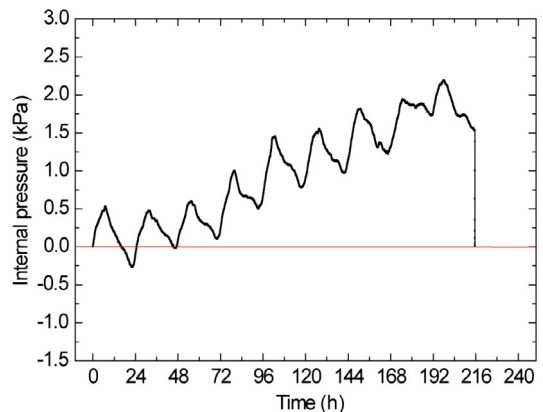


Fig. 9 Variation of internal pressure in a completely closed building model over 9 d

3.2 Nominally sealed building

Different numbers of small leakage holes opened on the surface of a completely closed building model

can be used to accurately simulate different background leakage ratios. If the original building model is not completely closed (i.e. has background leakage), the simulated background leakage ratio cannot be reliable. To accurately investigate the internal pressure responses in a nominally sealed building, the variation of the mean and peak internal pressure responses with different background leakage ratios was studied in the following wind tunnel experiments. The building model was first kept strictly completely closed and then some small leakage holes were opened on its surface to accurately simulate different background leakage ratios.

Fig. 10a demonstrates the variation of the mean internal pressure coefficient \bar{C}_{pi} with the relative leakage ratio ϕ_1 (the leakage ratio η on the leeward wall/the fixed leakage ratio $\eta=50\%$ on the windward wall). The variation of the mean internal pressure coefficient \bar{C}_{pi} with the relative leakage ratio ϕ_2 (leakage η on the windward wall/the fixed leakage ratio $\eta=50\%$ on the leeward wall) is shown in Fig. 10b. The results indicate that the variation of the mean internal pressure coefficient \bar{C}_{pi} with the relative leakage ratio for both small and large roofs was nearly the same. That is, the size of the building model had little influence on the mean internal pressure response in the nominally sealed building. Therefore, the next analysis focused on investigating internal pressure responses in the nominally sealed building with a small roof.

3.2.1 Probability density distribution

To determine a method for calculating the peak internal pressure coefficient, it is necessary to analyze the probability density distributions of fluctuating internal pressure coefficients. The probability density distribution curves are presented in Figs. 11 and 12 when the leakage ratio η of each wall was 50% and 100%, respectively. In both figures, the measured internal pressure coefficients were close to a standard Gaussian distribution. Statistics of skewness s and kurtosis k of the internal pressure coefficients in all the cases are shown in Fig. 13. The skewness values were concentrated from -0.5 to 0.5 and the kurtosis values from 2.5 to 3.5 , which are very similar to the corresponding values ($s=0$ and $k=3$) in a standard Gaussian distribution. As a result, the internal pres-

sure response in a nominally sealed building approximately obeys a Gaussian distribution and the peak internal pressure coefficient \hat{C}_{pi} can be determined by

$$\hat{C}_{pi} = \bar{C}_{pi} + g\tilde{C}_{pi}, \tag{5}$$

where g is a peak factor (2.5 and 3.5 are taken in later analysis).

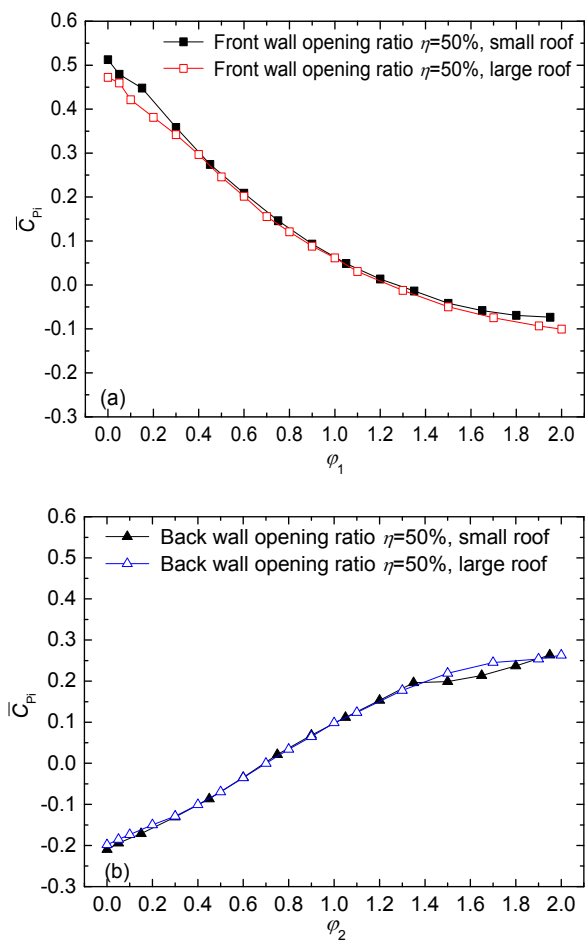


Fig. 10 Variation of the mean internal pressure coefficient \bar{C}_{pi} with the relative leakage ratio ϕ_1 (a) and the relative leakage ratio ϕ_2 (b)

3.2.2 Uniform background leakage distribution

A uniform background leakage distribution means that each wall of the building model has the same background leakage. Fig. 14 (p.495) demonstrates the variation of the mean and peak internal

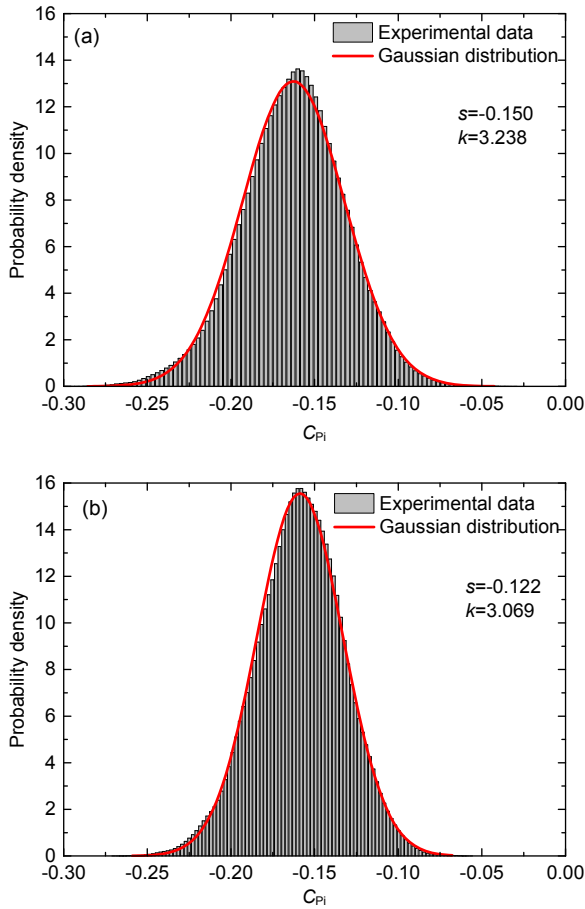


Fig. 11 Probability density distribution of fluctuating internal pressure when the leakage ratio $\eta=50\%$ with a wind direction of 0° (a) and 60° (b)

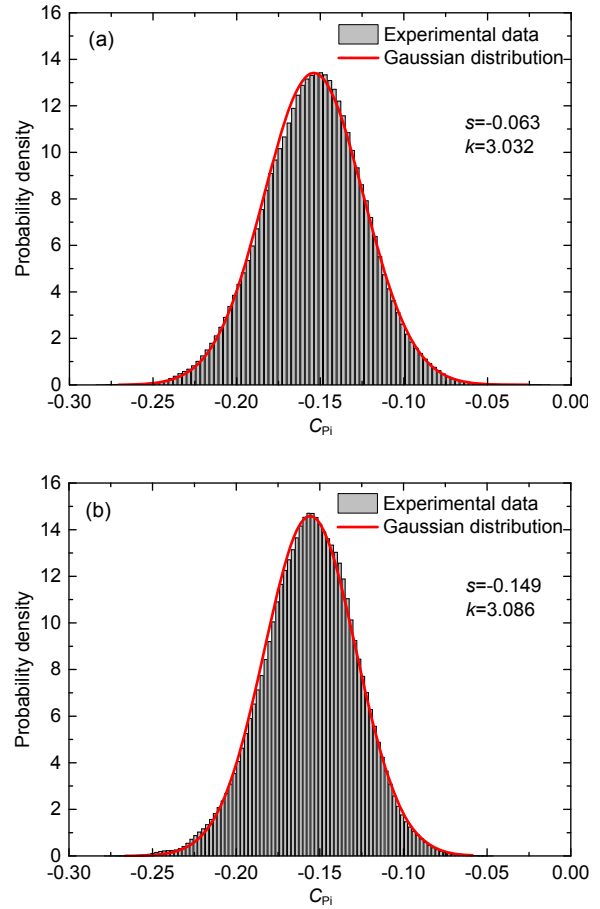


Fig. 12 Probability density distribution of fluctuating internal pressure when the leakage ratio $\eta=100\%$ with a wind direction of 0° (a) and 60° (b)

pressure coefficients with the absolute background leakage ratio ε . It can be seen that: (1) \bar{C}_{pi} varied within the range -0.15 – -0.14 with different absolute background leakage ratios, which indicates that the mean internal pressure coefficient remains unchanged with increasing background leakage. In addition, the mean internal pressure coefficients were negative and lower than the value of -0.2 suggested by the Chinese wind load code. (2) When the peak factor g was 2.5 or 3.5, the corresponding maximum peak values of the internal pressure coefficient under different absolute background leakage ratios ε were -0.063 and -0.033 , respectively, while the corresponding minimum values were -0.224 and -0.255 , respectively. The peak internal pressure coefficient did not change rapidly. According to the Chinese wind load code, the gust factor G is 1.63 at roof height, so the minimum peak internal pressure coefficient could be obtained as

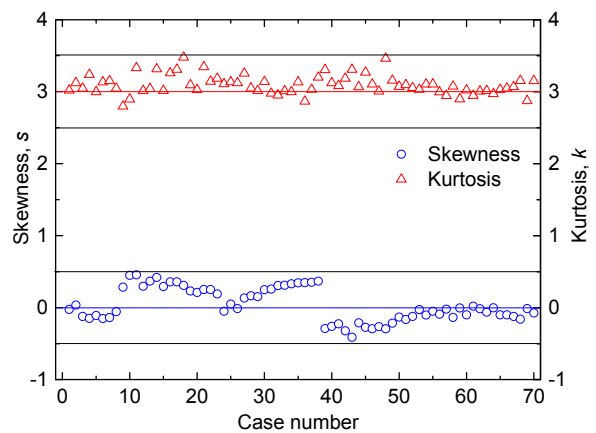


Fig. 13 Values of skewness and kurtosis in all cases

-0.245 from the equation $\hat{C}_{pi} = G\bar{C}_{pi}$. The calculated value of -0.245 was close to the wind tunnel-tested value of -0.255 when the peak factor g was 3.5,

which indicates lower magnitudes than the value of -0.326 suggested by the wind load code. This shows that the tested gust factor $G = \hat{C}_{pi} / \bar{C}_{pi} = (-0.224) / (-0.15) \approx 1.5$ in a nominally sealed building was smaller than that suggested by the wind load code.

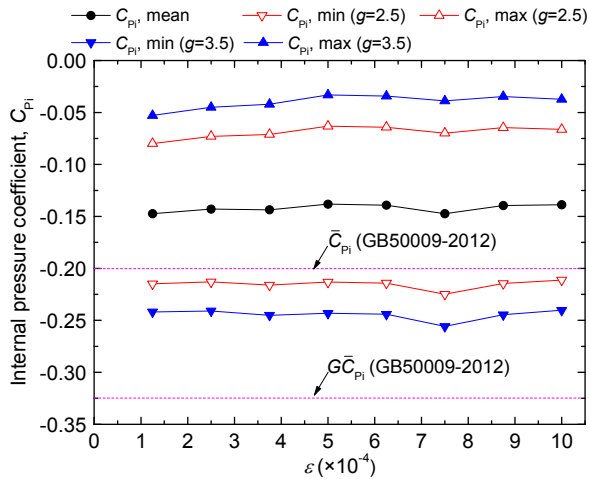


Fig. 14 Variation of the peak internal pressure coefficient with the absolute leakage ratio (cases 1–8)

3.2.3 Influence of wind direction

The effects of wind direction on internal pressure responses were investigated in wind tunnel experiments when the leakage ratio η on each wall was 100% or 50% (Fig. 15). Only wind directions from 0° to 90° were examined due to symmetry. It can be seen that: (1) \bar{C}_{pi} varied from -0.145 to -0.09 when the leakage ratio on each wall was 100%. The maximum value of $\bar{C}_{pi} = -0.09$ occurred with a wind direction of 90° , while the minimum value of $\bar{C}_{pi} = -0.145$ occurred with a wind direction of 45° . (2) The range of \bar{C}_{pi} was wider, varying from -0.17 to -0.11 when the leakage ratio on each wall was 50%, with a minimum value of -0.17 at a wind direction of 50° , and a maximum value of -0.11 at a wind direction of 90° . However, both values were lower than the value -0.2 suggested by the Chinese wind load code. (3) As for the peak internal pressure coefficient, the maximum positive value of the peak internal pressure coefficient failed to reach zero even when a higher peak factor $g=3.5$ was adopted, i.e. the peak internal pressure

coefficient remained negative at all wind directions. The minimum negative value of the peak internal pressure coefficient did not exceed -0.27 , which indicates a much lower magnitude than the value of -0.326 calculated by the wind load code.

3.2.4 Influence of relative leakage ratio

To investigate the effects of different wall leakages on internal pressure responses, the leakage ratio η of one wall was fixed while those of the other walls were changed in wind tunnel experiments. A relative leakage ratio ϕ (total leakage ratio η of the walls with changed holes/total leakage ratio η of the walls with fixed holes) was adopted to represent different background leakage distributions.

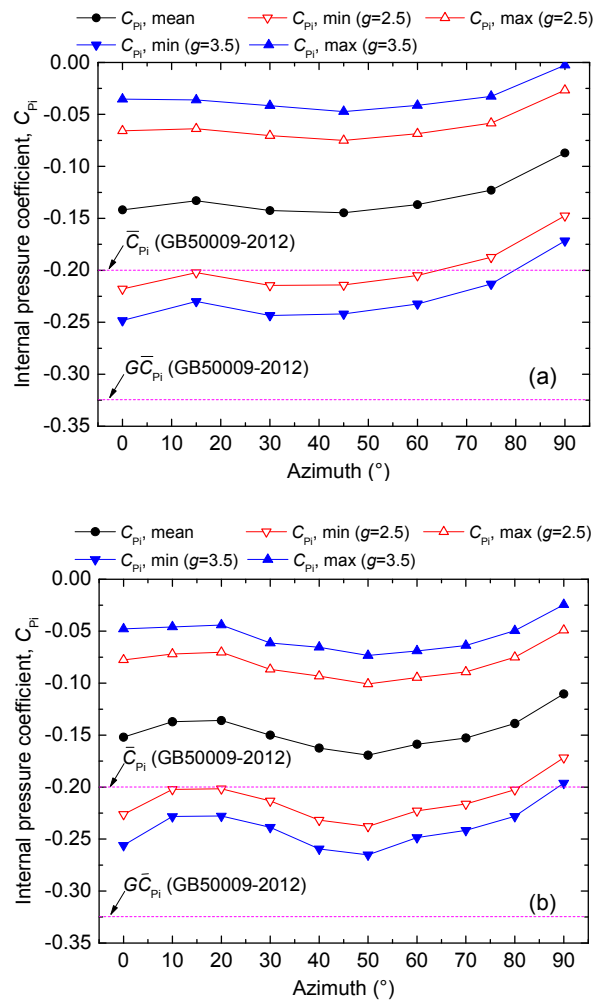


Fig. 15 Variation of internal pressure coefficient with wind direction when the leakage ratio on each wall was 100% (a) and 50% (b)

3.2.4.1 Fixed leakages on windward wall and no leakage on either sidewall

Variation of the mean and peak internal pressure coefficients with the relative background leakage ratio was studied by changing the leakage ratio η of the leeward wall under the condition that both sidewalls were completely closed and the leakage ratio η on the windward wall was fixed at 50%. The effects of the relative leakage ratio ϕ on both the mean and peak internal pressure coefficients were remarkable (Fig. 16). The most unfavorable situation occurred when the relative leakage ratio ϕ was zero, producing much higher mean and peak internal pressures. The mean internal pressure coefficient \bar{C}_{pi} reached its maximum value of 0.51 and the corresponding positive peak internal pressure coefficient reached 0.85 when the peak factor g was 3.5. In addition, both \bar{C}_{pi} and \hat{C}_{pi} decreased with increasing ϕ . \bar{C}_{pi} was close to zero when ϕ was 1.25, and then the internal pressure changed into suction and slowly decreased. When the relative leakage ratio ϕ was 2.0, \bar{C}_{pi} reached its minimum value of -0.07 , which indicates a much lower magnitude than the mean internal pressure coefficient $\bar{C}_{pi} = -0.15$ in the case of a uniform leakage distribution, and the minimum negative peak internal pressure coefficient was calculated as -0.2 by adopting $g=3.5$.

3.2.4.2 Fixed leakages on leeward wall and no leakage on either sidewall

Under the condition that both sidewalls were completely closed and the leakage ratio η on the leeward wall was fixed at 50%, the variation of the mean and peak internal pressure coefficients with the relative background leakage ratio ϕ is shown in Fig. 17, when the leakage ratio η of the windward wall changed from 0 to 1. Clearly, the variation trend was opposite to that presented in Fig. 16. \bar{C}_{pi} reached its minimum value of -0.21 when the relative leakage ratio ϕ was zero, and the corresponding negative peak internal pressure coefficient was -0.34 when the peak factor g was 3.5. Subsequently, both \bar{C}_{pi} and \hat{C}_{pi} increased with increasing ϕ , and \bar{C}_{pi} was close to zero when ϕ was 0.75. Then, the mean internal pressure changed from negative to positive and slowly

increased. The maximum value of \bar{C}_{pi} was 0.26 when ϕ was 2.0, i.e. all the windward leakage holes were opened, and the corresponding positive peak internal pressure coefficient was 0.5 when the peak factor g was 3.5.

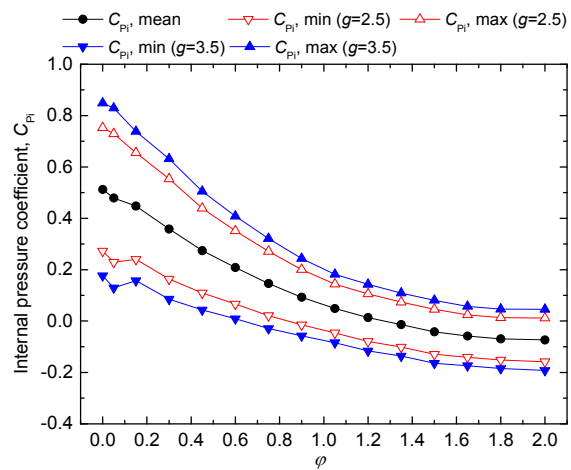


Fig. 16 Variation of the internal pressure coefficient with the relative leakage ratio (cases 9–13)

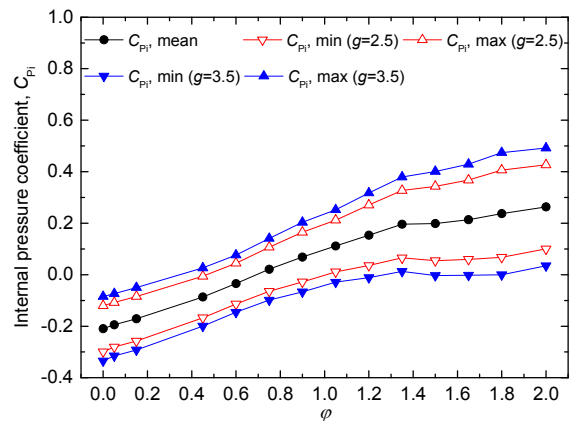


Fig. 17 Variation of the internal pressure coefficient with the relative leakage ratio (cases 24–38)

3.2.4.3 Fixed leakages on leeward wall and both sidewalls

When the leakage ratios η on the leeward wall and both sidewalls were all set at 100%, the variation of the mean and peak internal pressure coefficients with the relative leakage ratio ϕ was as shown in Fig. 18, when the leakage ratio η of the windward wall changed from 0 to 1. \bar{C}_{pi} varied within the range from -0.326 to -0.143 , and with an increasing trend.

The maximum and minimum values of \hat{C}_{pi} were obtained when φ achieved its maximum and minimum values, respectively. The maximum positive peak internal pressure coefficient failed to reach zero even when the peak factor g was adopted as 3.5. However, the minimum negative peak internal pressure coefficient reached -0.48 , which is higher than that when the leakage holes on both the windward wall and the sidewalls were completely closed and there were background leakage holes only on the leeward wall.

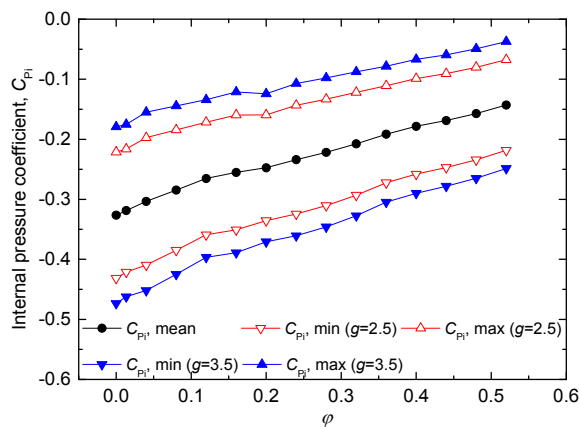


Fig. 18 Variation of the internal pressure coefficient with the relative leakage ratio (cases 39–53)

4 Conclusions

In this study, internal pressure characteristics were first investigated in a completely closed building model. Different numbers of small leakage holes were opened on the surface of the model to accurately simulate different background leakage ratios. Wind tunnel experiments were conducted to study the internal pressure response in a nominally sealed building model. The probability density distribution characteristics of fluctuating internal pressure were analyzed to determine a method to calculate peak internal pressure. The effects of uniform absolute leakage ratio, wind direction, and relative leakage ratio on the mean and peak internal pressure coefficients were examined in detail. The main conclusions are as follows:

1. Internal pressure in the completely closed building was non-stationary, and the internal pres-

ures collected at different time points varied significantly. A period of about 24 h was observed from the internal pressure time history sampled over 9 d.

2. The effect of building model dimensions on the mean internal pressure in a nominally sealed building may be negligible.

3. Wind-induced internal pressure in the nominally sealed building approximately obeyed a Gaussian distribution.

4. For the building with uniform background leakage on each wall, the mean internal pressure coefficient varied within the range from -0.15 to -0.14 , which indicates lower magnitudes than the value of -0.2 suggested by the Chinese wind load code (GB50009-2012). The minimum negative peak internal pressure coefficient was -0.255 when the peak factor was 3.5, which also indicates a lower magnitude than the value of -0.326 calculated from Chinese wind load code.

5. The maximum positive mean and peak internal pressures occurred only when background leakages appeared on the windward wall while the other walls were completely closed. The maximum positive mean internal pressure coefficient was 0.51, and the corresponding peak internal pressure coefficient reached 0.85 when the peak factor was 3.5.

6. The minimum negative mean and peak internal pressures occurred when the windward wall was completely closed while background leakages appeared on the other walls. The minimum negative mean internal pressure coefficient was -0.33 , and the corresponding peak internal pressure coefficient was -0.48 when the peak factor was 3.5.

Contributors

Zhuang-ning XIE and Xian-feng YU designed the research. Xian-feng YU processed the corresponding data. Jing-xuan GAO wrote the first draft of the manuscript. Xu WANG helped to organize the manuscript. Xian-feng YU revised and edited the final version.

Conflict of interest

Xian-feng YU, Jing-xuan GAO, Zhuang-ning XIE, and Xu WANG declare that they have no conflict of interest.

References

- Ginger JD, Mehta KC, Yeatts BB, 1997. Internal pressures in a low-rise full-scale building. *Journal of Wind Engineering and Industrial Aerodynamics*, 72:163-174.
[https://doi.org/10.1016/S0167-6105\(97\)00241-9](https://doi.org/10.1016/S0167-6105(97)00241-9)

- Guha TK, Sharma RN, Richards PJ, 2011. Internal pressure dynamics of a leaky building with a dominant opening. *Journal of Wind Engineering and Industrial Aerodynamics*, 99(11):1151-1161.
<https://doi.org/10.1016/j.jweia.2011.09.002>
- Guha TK, Sharma RN, Richards PJ, 2013a. Dynamic wind load on an internal partition wall inside a compartmentalized building with an external dominant opening. *Journal of Architectural Engineering*, 19(2):89-100.
[https://doi.org/10.1061/\(ASCE\)AE.1943-5568.0000113](https://doi.org/10.1061/(ASCE)AE.1943-5568.0000113)
- Guha TK, Sharma RN, Richards PJ, 2013b. Wind induced internal pressure overshoot in buildings with opening. *Wind and Structures*, 16(1):1-23.
<https://doi.org/10.12989/was.2013.16.1.001>
- Holmes JD, 1979. Mean and fluctuating internal pressures induced by wind. Proceedings of the 5th International Conference on Wind Engineering, p.435-450.
<https://doi.org/10.1016/B978-1-4832-8367-8.50046-2>
- Kopp GA, Oh JH, Incullet DR, 2008. Wind-induced internal pressures in houses. *Journal of Structural Engineering*, 134(7):1129-1138.
[https://doi.org/10.1061/\(asce\)0733-9445\(2008\)134:7\(1129\)](https://doi.org/10.1061/(asce)0733-9445(2008)134:7(1129))
- MOHURD (Ministry of Housing and Urban-Rural Development of the People's Republic of China), 2012. Load Code for the Design of Building Structures, GB50009-2012. National Standards of the People's Republic of China (in Chinese).
- Oh JH, Kopp GA, Incullet DR, 2007. The UWO contribution to the NIST aerodynamic database for wind loads on low buildings: part 3. Internal pressures. *Journal of Wind Engineering and Industrial Aerodynamics*, 95(8):755-779.
<https://doi.org/10.1016/j.jweia.2007.01.007>
- Pan F, Cai CS, Zhang W, 2013. Wind-induced internal pressures of buildings with multiple openings. *Journal of Engineering Mechanics*, 139(3):376-385.
[https://doi.org/10.1061/\(asce\)em.1943-7889.0000464](https://doi.org/10.1061/(asce)em.1943-7889.0000464)
- Saathoff PJ, Liu H, 1983. Internal pressure of multi-room buildings. *Journal of Engineering Mechanics*, 109(3):908-919.
[https://doi.org/10.1061/\(asce\)0733-9399\(1983\)109:3\(908\)](https://doi.org/10.1061/(asce)0733-9399(1983)109:3(908))
- Sharma RN, Richards PJ, 1997. Computational modelling in the prediction of building internal pressure gain functions. *Journal of Wind Engineering and Industrial Aerodynamics*, 67-68:815-825.
[https://doi.org/10.1016/S0167-6105\(97\)00121-9](https://doi.org/10.1016/S0167-6105(97)00121-9)
- Stathopoulos T, Luchian HD, 1989. Transient wind-induced internal pressures. *Journal of Engineering Mechanics*, 115(7):1501-1514.
[https://doi.org/10.1061/\(asce\)0733-9399\(1989\)115:7\(1501\)](https://doi.org/10.1061/(asce)0733-9399(1989)115:7(1501))
- Teclé AS, Bitsuamlak GT, Aly AM, 2013. Internal pressure in a low-rise building with existing envelope openings and sudden breaching. *Wind and Structures*, 16(1):25-46.
<https://doi.org/10.12989/was.2013.16.1.025>
- Yu SC, 2016. Wind tunnel study on vortex-induced Helmholtz resonance excited by oblique flow. *Experimental Thermal and Fluid Science*, 74:207-219.
<https://doi.org/10.1016/j.expthermflusci.2015.12.008>
- Yu SC, Lou WJ, Sun BN, 2006. Wind-induced internal pressure fluctuations of structure with single windward opening. *Journal of Zhejiang University-SCIENCE A*, 7(3):415-423.
<https://doi.org/10.1631/jzus.2006.A0415>
- Yu SC, Lou WJ, Sun BN, 2008. Wind-induced internal pressure response for structure with single windward opening and background leakage. *Journal of Zhejiang University-SCIENCE A*, 9(3):313-321.
<https://doi.org/10.1631/jzus.a071271>
- Yu XF, Quan Y, Gu M, 2012. Responses of wind-induced internal pressure in a two-compartment building with a dominant opening and background porosity part 1: theoretical formulation and experimental verification. *Journal of Central South University*, 19(10):2940-2948.
<https://doi.org/10.1007/s11771-012-1362-1>
- Yu XF, Gu M, Xie ZN, 2019. Linearized analysis of the internal pressures for a two-compartment building with leakage. *Wind and Structures*, 28(2):89-97.
<https://doi.org/10.12989/was.2019.28.2.089>

中文概要

题目: 名义封闭结构风致内压的试验研究

目的: 在确保模型气密性绝对良好的前提下, 通过设置不同的背景泄漏, 详细研究不同背景孔隙率和风向角下的平均和峰值内压水平, 为工程结构抗风设计和规范修订提供指导和依据。

创新点: 首次探究了完全封闭结构的内压特征, 并在此基础上系统研究了不同背景孔隙率和风向角下名义封闭结构的风致内压变化规律。

方法: 1. 在静态空气中进行压力测试, 获得完全封闭结构的内压特性(图 6~9)。2. 在完全封闭结构的表面开不同的孔隙; 通过多参数风洞试验(图 3 和表 1), 获得名义封闭结构的平均和峰值风压变化特征(图 14~18), 并与中国建筑结构荷载规范(GB50009-2012)进行对比分析。

结论: 1. 完全封闭结构的内压呈非平稳状态, 长达 9 d 的观察结果表明内压呈现一定的周期性。2. 在均布背景孔隙下, 平均内压系数仅在-0.15~-0.14 范围内波动, 且低于中国建筑结构荷载规范的取值-0.2。3. 当峰值因子 g 取 3.5 时, 最高负峰值风压系数为-0.255, 低于由规范计算得到的峰值内压系数-0.326。

关键词: 内压; 风洞试验; 完全封闭; 背景泄漏